

Four-Wave Mixing and Biphoton Generation in a Two-Level System

Shengwang Du,^{1,*} Jianming Wen,² Morton H. Rubin,² and G. Y. Yin¹

¹*Edward L. Ginzton Laboratory, Stanford University, Stanford, California 94305, USA*

²*Physics Department, University of Maryland, Baltimore County, Baltimore, Maryland 21250, USA*

(Received 4 October 2006; published 29 January 2007)

We find that in a two-level system there are two kinds of four-wave mixing processes which destructively contribute to the third-order nonlinear susceptibility. In a paired-photon generation scheme by using a single retroreflected pump beam, these two processes occur with definite time orders. The biphoton temporal correlation, which is measured with a back-to-back geometry in a laser-cooled two-level atomic ensemble, shows a damped Rabi oscillation and photon antibunching. Without suppressing the background of Rayleigh scattering, the upper limit of Cauchy criteria is estimated.

DOI: 10.1103/PhysRevLett.98.053601

PACS numbers: 42.50.Dv, 32.80.-t, 42.65.An, 42.65.Lm

Entangled photon generation has become one of the energetic research fields in quantum optics today. Traditionally, broadband paired photons are produced from spontaneous parametric down-conversion in a nonlinear crystal [1,2]. Recently, electromagnetically induced transparency has been used to generate narrow-band biphotons [3,4] which may have the potential application in the long-distance quantum communication [5]. An experimental examination of paired-photon generation using a four-wave parametric interaction in a two-level system with cold atoms is presented. This is in contrast to the previous work [6,7] conducted in either an atomic beam or a room-temperature cell with very low conversion efficiency. In this Letter, the emphasis is made on the underlying physics of the damped Rabi oscillation shown in the two-photon coincidences, which, to our best knowledge, are observed for the first time in a two-level atomic ensemble. Our simple perturbation theory is in agreement with the experiment.

Four-wave mixing (FWM) in a two-level system has been studied for more than 20 years [8,9]. In our study we find that there are two kinds of FWM processes which destructively contribute to the third-order nonlinear susceptibility $\chi^{(3)}$. In the limit of a large pump detuning Δ , $\chi^{(3)}$ is proportional to $1/\Delta^3$. However, in the paired-photon generation scheme, the two FWM processes occur with different time ordering. Their associated third-order nonlinear susceptibility is proportional to $1/\Delta^2$. The interference between triplet resonances leads to a damped Rabi oscillation in the two-photon temporal correlation.

First, we consider a conventional FWM experiment as shown in Fig. 1(a) where a pump laser propagates through a two-level atomic ensemble and is retroreflected by a mirror. The pump field has an angular frequency of $\omega_p = \omega_0 + \Delta$, where ω_0 is the on-resonance atomic transition frequency and Δ is the detuning. A third field with $\omega_3 = \omega_p + \delta$ is applied to generate its backward phase-matched field at $\omega_4 = \omega_p - \delta$. As depicted in Fig. 1(b), there are two FWM processes contributing to the generated field. To

derive the induced third-order nonlinear polarization, we begin with the atomic wave function $|\Psi; t\rangle = a_g(t)|g\rangle + a_e(t)e^{-i\omega_0 t}|e\rangle$. With the atom-field interaction $\hat{V}(t) = -\frac{1}{2}\hbar(\Omega_{p1}e^{i\omega_{p1}t} + \Omega_{p2}e^{i\omega_{p2}t} + \Omega_3e^{i\omega_3 t})|g\rangle\langle e| + \text{c.c.}$, the probability amplitudes can be perturbatively expanded as $a_g(t) = 1 + a_g^{(2)}(t) + \dots$ and $a_e(t) = a_e^{(1)}(t) + a_e^{(3)}(t) + \dots$, where $a_g^{(i)}$ and $a_e^{(i)}$ denote amplitudes of the i th order in the strength parameter of the interaction potential. Here Ω_{p1} and Ω_{p2} are the Rabi frequencies of the two counter-propagating pump beams, and Ω_3 is the Rabi frequency of the third field. The third-order (complex) polarization $P^{(3)}$ at frequency ω_4 is found to have two terms

$$\begin{aligned} P^{(3)} &= P_I^{(3)} + P_{II}^{(3)} \\ &= 2N\mu_{eg}[a_e^{(3)*}(\Omega_{p2}^*\Omega_3\Omega_{p1}^*) \\ &\quad + a_e^{(1)*}(\Omega_{p1}^*)a_g^{(2)}(\Omega_{p2}\Omega_3^*)], \end{aligned} \quad (1)$$

where N is the atomic density and μ_{eg} is the dipole matrix element. $P_I^{(3)}$ and $P_{II}^{(3)}$ represent the type (I) and (II) FWM processes shown in Fig. 1(b). Taking into account the dipole relaxation rate γ_e and ground state dephasing rate γ_g , the time-dependant perturbation theory gives:

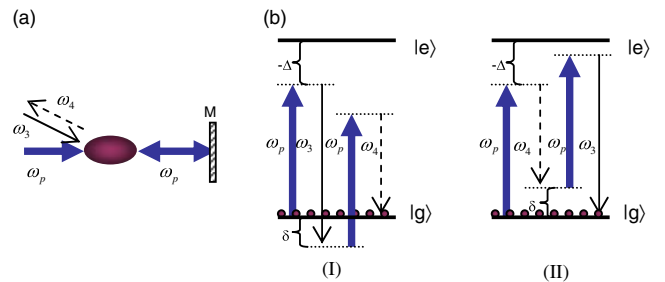


FIG. 1 (color online). Four-wave mixing (FWM) in a two-level system where the field $\omega_4 = 2\omega_p - \omega_3$ is generated. (a) Experimental configuration. (b) Two FWM processes which may produce the ω_4 field.

$$P_I^{(3)} = \frac{N\mu_{eg}\Omega_{p1}\Omega_{p2}\Omega_3^* e^{i(\omega_p - \delta)t}}{4(\Delta - i\gamma_e)(\Delta - \delta - i\gamma_e)(\delta + i\gamma_g)}, \quad (2)$$

$$P_{II}^{(3)} = -\frac{N\mu_{eg}\Omega_{p1}\Omega_{p2}\Omega_3^* e^{i(\omega_p - \delta)t}}{4(\Delta - i\gamma_e)(\Delta + \delta + i\gamma_e)(\delta + i\gamma_g)}. \quad (3)$$

As we see, $P_I^{(3)}$ has two resonances at $\delta = 0$ and $\delta = \Delta$. $P_{II}^{(3)}$ has two resonances at $\delta = 0$ and $\delta = -\Delta$. Equations (2) and (3) together give the so-called triplet-resonance structure. The “-” sign in (3) indicates a destructive interference in the total nonlinear polarization $P^{(3)}$:

$$P^{(3)} = \frac{N\mu_{eg}\Omega_{p1}\Omega_{p2}\Omega_3^* e^{i(\omega_p - \delta)t}(\delta + i\gamma_e)}{2(\Delta - i\gamma_e)(\Delta - \delta - i\gamma_e)(\Delta + \delta + i\gamma_e)(\delta + i\gamma_g)}. \quad (4)$$

Equation (4) is a standard formula in nonlinear optics which is proportional to $1/\Delta^3$ in the limit of large detuning [8,9]. In traditional FWM experiments with three classical input fields that have no time order defined, the two processes shown in Fig. 1(b) should be added together to give the spectrum of the ω_4 field, and the central component is thus suppressed in $P^{(3)}$.

We now turn to the main part of this Letter. In the presence of a retroreflected pump beam, counterpropagating correlated photons (ω_3 and ω_4) are produced spontaneously [Fig. 2(a)]. The photon pairs are created with a definite time order; for example, as shown in Fig. 2(b), the ω_3 photon is radiated before the ω_4 photon. By measuring the time delay between them, we know from which transition path in Fig. 2(b) the single photons are coming. As a consequence, to describe the biphoton generation, the third-order polarization should be decomposed by following the time order. In other words, for photons at frequencies of ω_3 and ω_4 , the third-order nonlinear polarizations are represented by $P_{II}^{(3)}$ and $P_I^{(3)}$, respectively. The third-order nonlinear susceptibilities associated with the ω_3 and ω_4 fields are then equivalently given by:

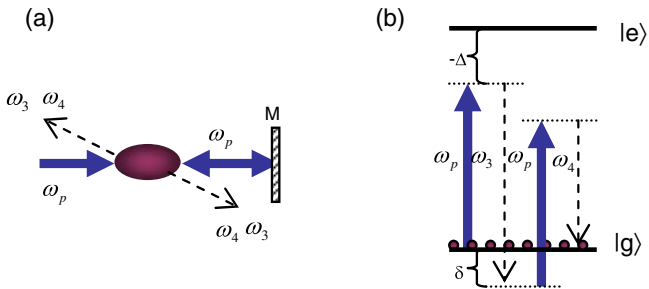


FIG. 2 (color online). Schematic of spontaneous paired-photon generation in a two-level system. (a) Simplified experimental configuration. (b) The parametric process which generates the frequencies at ω_3 and ω_4 .

$$\chi_3^{(3)}(\delta) = \frac{-N|\mu_{eg}|^4}{4\hbar^3\epsilon_0} \frac{1}{(\Delta - i\gamma_e)(\Delta - \delta + i\gamma_e)(-\delta + i\gamma_g)}, \quad (5)$$

$$\chi_4^{(3)}(-\delta) = \frac{N|\mu_{eg}|^4}{4\hbar^3\epsilon_0} \frac{1}{(\Delta - i\gamma_e)(\Delta - \delta - i\gamma_e)(\delta + i\gamma_g)}. \quad (6)$$

The propagation of the generated fields is governed by the Maxwell's equations. Working in the Heisenberg picture, under the slowly varying amplitude approximation, the field operators \hat{a}_3 and \hat{a}_4 obey

$$\frac{\partial \hat{a}_3}{\partial z} + \left[\alpha_3(\delta) + \frac{i\Delta k}{2} \right] \hat{a}_3 - \kappa_3(\delta) \hat{a}_4^\dagger = \hat{\mathcal{F}}_3, \quad (7)$$

$$\frac{\partial \hat{a}_4^\dagger}{\partial z} + \left[\alpha_4(-\delta) - \frac{i\Delta k}{2} \right] \hat{a}_4^\dagger - \kappa_4(-\delta) \hat{a}_3 = \hat{\mathcal{F}}_4, \quad (8)$$

where

$$\begin{aligned} \alpha_3(\delta) &= -\frac{i\omega_3 N |\mu_{eg}|^2}{2c\epsilon_0\hbar} \frac{1}{\Delta + \delta - i\gamma_e}, \\ \alpha_4(-\delta) &= -\frac{i\omega_4 N |\mu_{eg}|^2}{2c\epsilon_0\hbar} \frac{1}{\Delta - \delta + i\gamma_e}, \\ \kappa_3(\delta) &= \frac{-i\omega_3}{2c} \chi_3^{(3)}(\delta) E_p^2, \\ \kappa_4(-\delta) &= \frac{-i\omega_4}{2c} \chi_4^{(3)*}(-\delta) E_p^{*2}, \end{aligned} \quad (9)$$

and $\Delta k = 2\delta/c$ is the phase mismatch. $\hat{\mathcal{F}}_{3,4}$ are quantum Langevin noise operators, and $\alpha_{3,4}$ are the linear optical response. Clearly, the nonlinear coupling coefficients κ_3 and κ_4 are different from those in classical FWM [8,9] in the two-level systems.

Before solving the coupled Eqs. (7) and (8), it is instructive to examine the biphoton wave packet. In the limits of a large pump detuning and a weak optical excitation, by ignoring the absorption (or gain) and phase mismatch, to the first order the solution to Eq. (7) can be reduced to $\hat{a}_3(\delta) \simeq \kappa_3(\delta) L \hat{a}_4^+(-\delta)$. The biphoton wave packet in the time domain is a Fourier transform

$$\begin{aligned} \Psi_{34}(\tau = t_4 - t_3) &= \frac{1}{2\pi} \int \kappa_3(\delta) L e^{i\delta\tau} d\delta \\ &= W [e^{-\gamma_g\tau} - e^{i\Delta\tau} e^{-\gamma_e\tau}] \theta(\tau), \end{aligned} \quad (10)$$

where $\theta(\tau)$ is the Heaviside function and

$$W = \frac{\text{OD} \times \Omega^2 \gamma_e}{8(\Delta - i\gamma_e)(\Delta + i\gamma_e - i\gamma_g)}. \quad (11)$$

Here $\text{OD} = N\sigma_0 L$ is the optical depth with the on-resonance cross section $\sigma_0 = \frac{2\pi|\mu_{eg}|^2}{\epsilon_0\hbar\lambda\gamma_e} = \frac{\lambda^2}{2\pi}$, and Ω is the pump Rabi frequency. The Heaviside function $\theta(\tau)$ shown in Eq. (10) reveals that the ω_4 photon is radiated after the ω_3 photon. The two-photon coincidence counting rate is

the squared modulus of Eq. (10), i.e.,

$$R_{34} = |W|^2 [e^{-2\gamma_g\tau} + e^{-2\gamma_e\tau} - 2e^{-(\gamma_g+\gamma_e)\tau} \cos\Delta\tau] \theta(\tau). \quad (12)$$

Equation (12) displays photon antibunching [10] at $\tau = 0$. The damped oscillation with a frequency of Δ results from the interference between two resonance bands at $\delta = 0$ and Δ . The results obtained above are also consistent with a single atom picture: after the emission of a photon at ω_3 , the atom takes a Rabi period ($2\pi/\Delta$) to radiate a second one at ω_4 . In an atomic ensemble, the Rabi oscillation signals are amplified collectively because $|W|^2 \propto \text{OD}^2$. Considering the detection geometry, the biphoton wave packet and two-photon coincidence counting rate at the two detectors are expressed by $\Psi(\tau) = \Psi_{34}(\tau) + \Psi_{34}(-\tau)$ and $R(\tau) = R_{34}(\tau) + R_{34}(-\tau)$.

The experiment is done with cold atoms in a ^{87}Rb magneto-optical trap (MOT) at Stanford University [4]. The ^{87}Rb D2 line transition diagram and experimental configuration are shown in Fig. 3. By turning off the MOT trapping laser while keeping the repump laser on, the atoms are prepared at the ground level $|5S_{1/2}, F=2\rangle$. Then, in the presence of a retroreflected pump beam, phase-matched counterpropagating photon pairs are generated into opposing single-mode fibers and detected by single photon-counting modules (SPCM). The experiment was done periodically so as to create a 10% duty cycle, with the MOT process for 4.5 ms followed by an experimental window of 500 μs . The trapping magnetic field (10 G/cm) and repump laser remain on throughout the experiment. The pump laser, blue-detuned Δ from the cycle transition $|5S_{1/2}, F=2\rangle \rightarrow |5P_{3/2}, F'=3\rangle$, is chosen to be linearly polarized as shown in Fig. 3, collimated to a diameter of 1.6 mm and completely overlaps the atomic cloud. The pump transition has a natural linewidth

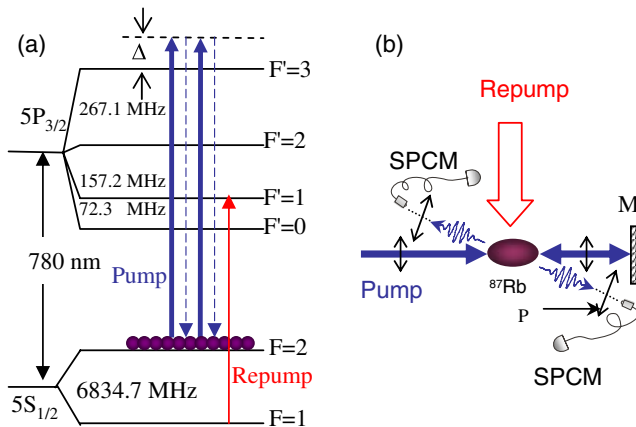


FIG. 3 (color online). (a) ^{87}Rb D2 line hyperfine energy-level diagram and (b) schematic of the experiment for paired-photon generation in a two-level system. In the presence of a linearly polarized, retroreflected pump beam, counterpropagating paired photons are produced into opposing single-mode fibers after linear polarizers (P).

of $\gamma_e/\pi = 6$ MHz. The fiber-fiber axis is 2 degrees from the pump beam direction. The atomic cloud has a length of about 1.5 mm and an OD of 12.7. Correlation statistics are binned into 512-bin histograms with a bin width of 1 ns. The joint detection efficiency in the two-photon coincidence measurement is about 10%.

Figure 4 shows the two-photon coincidence counts as a function of the time delay τ between detected photons. The theoretical curves (solid line, black) are obtained by solving the coupled Eqs. (7) and (8) numerically. To fit the experimental data, the biphoton coincidences are scaled by a factor of [0.31, 0.46, 0.25, 0.35] in Figs. 4(a)1, 4(a)2, 4(b)1, and 4(b)2, respectively. The flat background is due to the linear Rayleigh scattering. We have replaced the

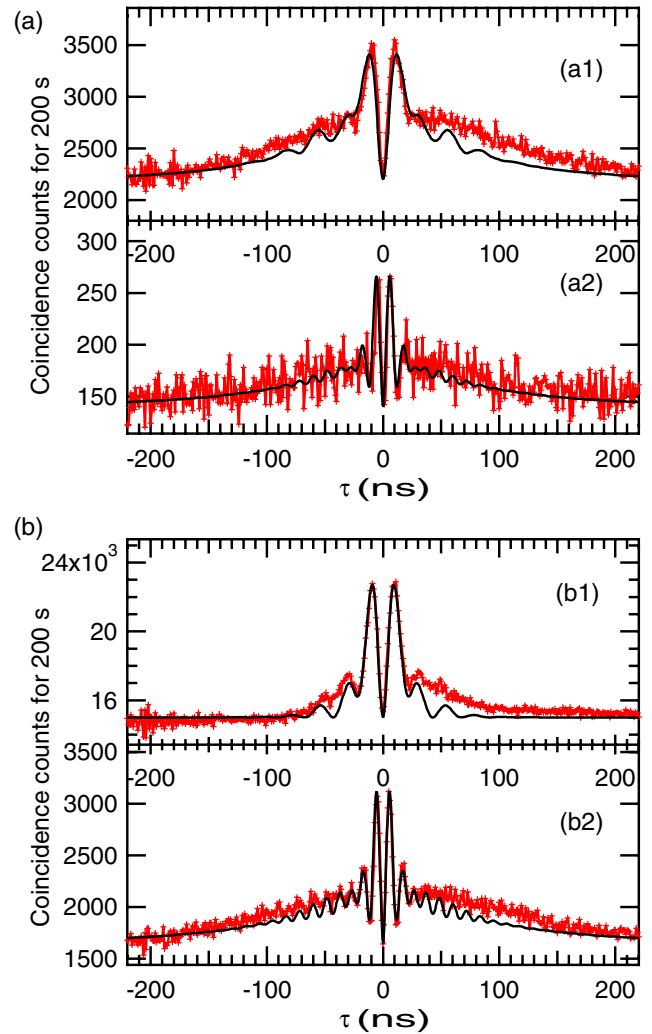


FIG. 4 (color online). Coincidence counts as a function of the time delay τ between detected photons. Experimental data (\dagger , red) was collected over 200 s. Theoretical curves (solid, black) are scaled by a factor of 0.31, 0.46, 0.25, and 0.35 from (a1) to (b2), respectively. (a) Pump power 250 μW : (a1) $\Delta/2\pi = 35.6$ MHz, $\gamma_g = 0.4\gamma_e$; (a2) $\Delta/2\pi = 83.6$ MHz, $\gamma_g = 0.3\gamma_e$. (b) Pump power 770 μW : (b1) $\Delta/2\pi = 35.6$ MHz, $\gamma_g = 2\gamma_e$; (b2) $\Delta/2\pi = 83.6$ MHz, $\gamma_g = 0.3\gamma_e$.

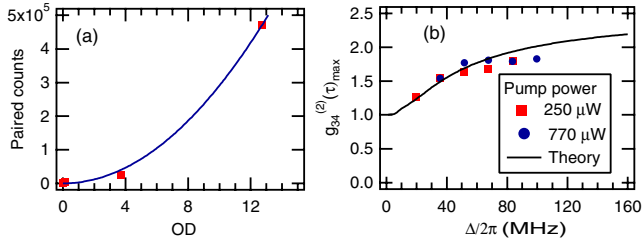


FIG. 5 (color online). (a) Number of total paired counts for 200 s vs optical depth (OD) with a pump power of 770 μW and a detuning of $\Delta/2\pi = 35.6$ MHz. (b) Maximum of the normalized second-order quantum coherence function $g_{34}^{(2)}(\tau)_{\text{max}}$ vs pump detuning Δ . The theoretical curve (solid, black), which is dependant of pump power, is calculated with $\gamma_g = 0.4\gamma_e$.

pump detuning Δ with the effective Rabi frequency $\Omega_e = \sqrt{\Omega^2 + \Delta^2}$ to take into account the power-broadening of the spectrum. The different scaling factors may result from the disturbance of the atomic cloud caused by the blue-detuned pump beams which heat and push the atoms. At a detuning of $\Delta/2\pi = 19.6$ MHz, we observe that the atomic cloud is completely destroyed by the pump beams at a power of 770 μW , while at a power of 250 μW , we still obtain paired counts. The fitted dephasing rate for a low pump power and large detuning gives a constant number $\gamma_g = 0.3\gamma_e = 2\pi \times 0.9$ MHz, corresponding to the long coherent tails ($1/2\gamma_g \sim 100$ ns) as shown in Fig. 4. This is consistent with the effective dephasing rate ($2\pi \times 1.0$ MHz) which we estimate from the pump laser linewidth (~ 300 kHz), MOT temperature (~ 300 kHz), and inhomogeneous magnetic field broadening (~ 1.4 MHz). The theory agrees well with the experiment and both show the damped Rabi oscillation in the two-photon temporal correlation. At the pump power of 770 μW and detuning of 35.6 MHz, the paired-photon generation rate is around $2 \times 10^5/\text{s}$.

Figure 5(a) shows that the measured coincidence counts is proportional to OD^2 . This indicates a collective contribution of the atomic ensemble. Figure 5(b) plots the measured maximum value of the normalized second-order quantum coherence function, $g_{34}^{(2)}(\tau)_{\text{max}}$, versus the pump detuning. In the limit of large detuning, $g_{34}^{(2)}(\tau)_{\text{max}}$ approaches a constant. With the measured autocorrelation functions $g_{33}^{(2)}(0) = g_{44}^{(2)}(0) = 2$, we find that the Cauchy-Schwartz inequality $[g_{34}^{(2)}(\tau)_{\text{max}}]^2/[g_{33}^{(2)}(0)g_{44}^{(2)}(0)] \leq 1$ is never violated within our experimental scope. The theoretical curve in Fig. 5(b) shows the possibility to violate the Cauchy criteria at a larger pump detuning. To see how the inequality is violated at a large detuning, we evaluate the Rayleigh scattering rate into a single-mode fiber as $S = \text{OD} \times \Omega^2 \gamma_e / [8(\Delta^2 + \gamma_e^2 + \Omega^2)]$. In the large pump-detuning limit, ignoring the absorption, one can find that

$g_{34}^{(2)}$ has a limitation $g_{34}^{(2)}(\tau) = 1 + R_{34}(\tau)/S^2 < 1 + 4|W|^2/S^2 \approx 5$, which also sets an upper limit for the Cauchy criteria.

In conclusion, using time-dependant perturbation theory, we find that there are two types of FWM processes which destructively contribute to the third-order nonlinearity in a two-level system. In the paired-photon generation, these two processes are present with definite time orders. $\chi_{3,4}^{(3)}$ together show the triplet-resonance structure; in the classical FWM, the central resonance is usually suppressed. Thus the coupled field equations have different nonlinear coupling coefficients from the classical FWM equations [12]. The interference of correlations from the central and side bands leads to a damped Rabi oscillation and photon antibunching. The theory agrees well with the experiment including the propagation effect. Moreover, we find that the Cauchy criteria has an upper limit because of the Rayleigh scattering. We have not seen any violation of the inequality within our experimental parameters. For a detailed theoretical analysis, see our continuing work [11].

The authors thank P. Kolchin, C. Belthangady, Y.-H. Shih, J. D. Franson, T. Pittman, and R. Y. Chiao for helpful discussions. The work was supported by the Defense Advanced Research Projects Agency, the US Air Force Office of Scientific Research, and the US Army Research Office. J. Wen and M. H. Rubin were supported in part by the US ARO MURI Grant No. W911NF-05-1-0197.

*Electronic address: dus@stanford.edu

- [1] S. E. Harris *et al.*, Phys. Rev. Lett. **18**, 732 (1967); D. Burnham and D. Weinberg, *ibid.* **25**, 84 (1970).
- [2] M. H. Rubin *et al.*, Phys. Rev. A **50**, 5122 (1994).
- [3] V. Balić *et al.*, Phys. Rev. Lett. **94**, 183601 (2005); C. H. van der Wal *et al.*, Science **301**, 196 (2003); J. K. Thompson *et al.*, *ibid.* **313**, 74 (2006); A. Kuzmich *et al.*, Nature (London) **423**, 731 (2003).
- [4] P. Kolchin, S. Du, C. Belthangady, G. Y. Yin, and S. E. Harris, Phys. Rev. Lett. **97**, 113602 (2006).
- [5] L.-M. Duan *et al.*, Nature (London) **414**, 413 (2001).
- [6] J. Dalibard and S. Reynaud, J. Phys. (France) **44**, 1337 (1983); P. Grangier *et al.*, Phys. Rev. Lett. **57**, 687 (1986); A. Aspect *et al.*, *ibid.* **45**, 617 (1980).
- [7] M. W. Mitchell *et al.*, Phys. Rev. A **62**, 043819 (2000).
- [8] R. W. Boyd, *Nonlinear Optics* (Academic, New York, 1992); R. W. Boyd *et al.*, Phys. Rev. A **24**, 411 (1981).
- [9] J. Nilsen and A. Yariv, Appl. Opt. **18**, 143 (1979).
- [10] D. F. Walls, Nature (London) **280**, 451 (1979); H. J. Kimble *et al.*, Phys. Rev. Lett. **39**, 691 (1977).
- [11] J. Wen, S. Du, and M. H. Rubin, Phys. Rev. A (to be published).
- [12] Considering the classical fields as entangled coherent radiation states shown in Fig. 1(b), the classical FWM field coupled equations can be derived from the operator coupled Eqs. (7) and (8).